Shear-speed gradients and ocean seismo-acoustic noise resonances

Oleg A. Godin[a)]
School of Earth and Ocean Sciences, University of Victoria, P.O. Box 3055, Victoria, British Columbia V8W 3P6, Canada

David M. F. Chapman
Defence Research Establishment Atlantic, P.O. Box 1012, Dartmouth, Nova Scotia B2Y 3Z7, Canada

(Received 10 September 1998; revised 10 June 1999; accepted 16 June 1999)

Measurements of infrasonic seismo-acoustic ambient noise using an ocean bottom seismometer in shallow water have uncovered an unusual phenomenon: the noise spectrum of the horizontal component of seabed velocity shows several prominent peaks in the frequency range 0–8 Hz, whereas the noise spectra of both the acoustic pressure and the vertical component of seabed velocity show very weak or nonexistent features at the same frequencies. This structure is interpreted theoretically as resonances of shear waves of vertical polarization in the upper sediment layer, excited by the diffuse infrasonic sound field in the water. Independent interface wave dispersion studies at the site have revealed an approximate power-law profile of shear speed versus depth, having the form $c(z)=c_0 z^{\nu}$, with $c_0=21.5$ and $\nu=0.60$ (SI units). The theoretical development concentrates on exact analytic solutions for the resonance frequencies and wave field for power-law profiles and on the WKB and more advanced asymptotic solutions in the more general case of smooth shear-speed profiles with a power-law singularity. The experimental observations are interpreted in light of these analytic results, and are consistent with the previously determined power-law shear speed-profile. © *1999 Acoustical Society of America.*
[S0001-4966(99)04110-7]

PACS numbers: 43.20.Gp, 43.25.Gf, 43.28.Dm, 43.30.Ma [DLB]

INTRODUCTION

Shear waves in marine sediments have proved to be a significant factor in bottom-interacting ocean acoustics in some environments.[1] Specifically, Hughes *et al.*[2] have shown that shear wave resonances in a thin sediment layer over a rock substrate have a profound effect on acoustic reflection loss and shallow water acoustic transmission loss. In that study, it was adequate to model the thin sediment layer as a single homogeneous layer with average properties; however, others have argued that gradients in material properties cannot be ignored.[3–5] This paper presents experimental evidence of a seabed resonance phenomenon involving shear waves in surficial sediments for which the theoretical explanation depends critically on the shear-speed gradient; the paper also proposes a wave-theoretical model for the phenomenon. The experiment consisted simply of measuring the seismo-acoustic ambient noise field at the seabed using an ocean bottom seismometer (OBS). The OBS was equipped with geophones for measuring the particle velocity at the top of the sediment layer and a hydrophone for measuring the pressure in the water layer just above. Interestingly, we observed large resonance effects on the horizontal geophone, but these resonances were absent on the hydrophone. In this paper, we are not so concerned with the seismo-acoustic noise field itself, its source mechanisms, or modeling its spectrum; these topics are covered in a good review by Orcutt *et al.*[6] and a recent monograph by Kibblewhite and Wu.[7] We are more interested in how the noise field interacts with the seabed, and the insight this provides into the seismo-acoustics of the seafloor.

A preliminary computational investigation[8] of this phenomenon using a stacked-layer geoacoustic model approximating a continuous power-law shear-speed profile of the form $c(z)=c_0 z^{\nu}$ provided encouraging results. However, we found that results converged slowly as the number of layers increased. It appears that prohibitively large numbers of layers would be necessary to adequately model the physics of such a profile using this method. Accordingly, in this paper we abandon the stacked-layer approach in favor of analytic treatment, returning to the fundamental equations of motion of acoustic waves in a continuously stratified elastic medium. These equations are difficult to solve exactly, but the low shear speeds present in the upper sediment layer of the experimental site admit a simplifying assumption that opens an avenue for an approximate analytical solution of the equations of motion. The analytic results provide characteristic equations for the expected resonance frequencies. Numerical solution of the resonance conditions is straightforward, and provides much insight into the observed ambient noise structure.

In Sec. I we present the experimental data showing the seafloor noise resonances and a description of the environment. In Sec. II we relate the noise resonances to normal modes of *P-SV* waves and indicate the small parameters of the problem that allow its analytical consideration. It is es-

[a)]Also affiliated to: Acoustic Wave Propagation Laboratory, P. P. Shirshov Oceanography Institute of the Russian Academy of Sciences, Moscow 117851, Russia.

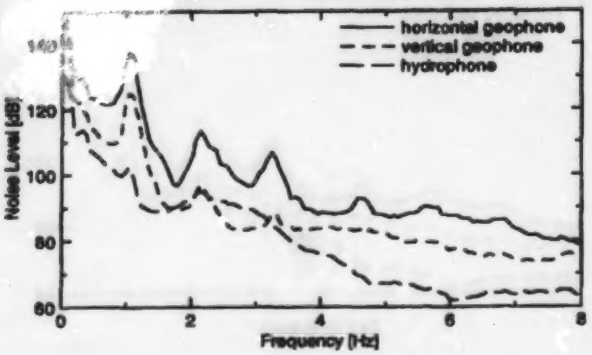

FIG. 1. Seismo-acoustic ambient noise resonances measured using an ocean bottom seismometer in a shallow-water site on the Scotian shelf. (Noise level units are dB *re*: 1 $(\text{nm/s})^2/\text{Hz}$ for the geophones and dB *re*: 1 $\mu\text{Pa}^2/\text{Hz}$ for the hydrophone.)

tablished in Sec. III that analysis of the normal modes at normal incidence provides sufficient accuracy to determine resonance frequencies. An exact solution for shear wave normal modes in a layer with power-law profile of rigidity is obtained and analyzed in Sec. IV. Effects of deviations from the power law are addressed in Sec. V. We provide some computational results in Sec. VI, to illustrate some of the analytically derived conclusions. Finally, in Sec. VII, we examine the interplay of the various model parameters, the most significant being the profile of shear speed versus depth in the sediment.

I. EXPERIMENT: RESONANCES IN SEISMO-ACOUSTIC AMBIENT NOISE

In 1993, the Defence Research Establishment Atlantic (DREA) built and tested an OBS to investigate the geophone as a sensor for ocean acoustics experiments.[9–11] Many experimental sites were visited on several cruises, including a site on the Scotian Shelf not far from the Eastern Shore coastal region of Nova Scotia. Seismo-acoustic propagation, ambient noise, and interface wave experiments were conducted at this site. The interface wave dispersion data (i.e., group speed versus frequency) were inverted to produce a shear speed versus depth profile in the seabed.[12] The site is located in a basin whose water depth is about twice as deep as the surrounding sand banks, and whose surficial sediment is composed of ponded layers of clay and silt over a harder material, probably glacial till.[12,13] Shear velocity in the hard sediment is estimated to be 900–1000 m/s. The water depth is 156 m and the clay/silt layer is about 25.5 m thick. The shear-speed profile was modeled as a stack of homogeneous sub-layers, but the resulting staircase could be viewed as an approximation to a continuous power-law profile of the form $c(z)=c_0 z^{\nu}$, with $c_0=21.5$ and $\nu=0.60$ (SI units), the shear speed varying from 21.5 m/s at 1 m depth to 150 m/s at the top of the till layer at 25.5 m depth.

Of particular interest in this paper are the resonance features in the seismo-acoustic ambient noise measured by the OBS on the seabed, shown in Fig. 1. We observed these features with the DREA OBS on two visits, but we initially saw them with a borrowed OBS of different design; this is persuasive evidence that the phenomenon is not an instrument effect. The resonances in the noise on the horizontal geophone are quite noticeable: the first five peaks are at 1.06, 2.16, 3.24, 4.64, and 5.70 Hz, the sequence closely approximating a harmonic progression with a fundamental frequency of 1.11 ± 0.04 Hz. (Later we show that the nonharmonic progression $1.18n-0.21$ is a better fit to this sequence.) Only one horizontal geophone channel is shown; the others are similar. The vertical geophone channel displays similar features, but they are much weaker, showing only the first three peaks. On the hydrophone channel, there is only a suggestion of a resonance at the fundamental frequency. We have not observed such resonances at other sites we visited with the DREA OBS; however, Dorman *et al.*[14] published OBS noise spectra from an entirely different location showing noticeable peaks on the horizontal geophone in the same frequency band (with a smoother and quieter noise spectrum on the vertical geophone), but they did not remark on the features.

The cause of these noise resonances was not immediately evident. At first, we suspected them to be instrument related, but their appearance at the same site at different times with different instruments convinced us that they are environmental features. We now believe that these peaks in the horizontal motion are caused by vertically polarized shear waves resonating in the clay/silt layers. At this time, we do not have a complete model of the phenomenon, but the following sections will examine seismo-acoustic propagation in this environment and the role of the shear-speed profile in placing the modeled resonances at the appropriate frequencies.

II. QUALITATIVE CONSIDERATIONS AND APPROACH

Our hypothesis to explain the observed features of the seismo-acoustic noise field assumes that the water column supports a diffuse infrasonic noise field that is horizontally isotropic, but which may have some vertical directionality. This noise field interacts with the elastic seabed, generating vertically polarized shear waves (*SV* waves). Previous analysis of similar problems suggests that the strongest generation of shear waves would occur at the large impedance contrast at the sediment/substrate boundary.[15] Subsequent multiple transits of the sediment layer by the shear waves give rise to resonances at frequencies that favor constructive interference. (Note that the lower boundary is necessary both to generate the shear waves and to provide a distinct layer thickness to form the resonances.) According to Snell's law, for very slow shear speeds the sediment-borne *SV* waves excited by water-borne sources would travel in an almost vertical direction, insensitive to the incidence angle of the wave in the water. Also, for very low shear speeds, there would be a negligible effect on the bottom reflection coefficient, hence we would not expect the hydrophone to register large resonance effects. However, the geophones of an OBS are capable of sensing the underlying seabed motion associated with shear waves, so resonances would be seen in the

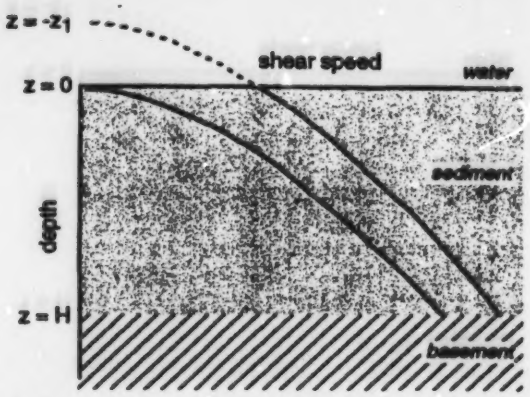

FIG. 2. Simple and truncated power-law shear-speed profiles in the sediment layer.

geophone ambient noise, although they should be more noticeable on the horizontal geophone signals than on the vertical geophones, as we explain below.

It is the low shear-wave velocities that are responsible for predominantly horizontal particle motion in vertically polarized shear waves. According to the Snell's law, sound waves incident from the water column give rise to shear waves that propagate almost vertically. Being transverse waves, these create almost-horizontal particle displacement. In addition, the shear-wave particle motion at the water/sediment boundary is the sum of an upward-traveling incident shear wave and a downward-traveling reflected shear wave. For low shear speeds, the shear wave is almost perfectly reflected with a phase inversion. This gives rise to a net displacement that is large in the horizontal direction and further reduced in the vertical direction.

Conventionally, numerical simulations of acoustic propagation in a stratified elastic medium are performed by subdividing the inhomogeneous layer into a number of homogeneous sub-layers. Although layer-stack models are remarkably versatile, they ultimately need a large number of sub-layers to model a depth interval where the shear velocity is small but its gradient is large, which is a characteristic feature of the environment at hand. Moreover, as noted in Ref. 5, "the layer-stack method presents no expression that yields insight into the effects being studied." In this paper, we abandon the assumption of piecewise constant medium parameters and consider the upper portion of the sediment to be a *continuously stratified* solid. The shear modulus of marine sediments is small in the vicinity of the water-sediment interface and may vanish at the interface. Then it is natural to assume a power-law dependence

$$\mu=\rho_0 c_0^2(z+z_1)^{2\nu}, \quad \nu>0, \quad z_1\geqslant 0 \tag{1}$$

of shear modulus on depth in the upper portion of the sediment column. Here ρ_0 is a constant with the dimensions of density ρ and c_0=const. There is both theoretical and empirical evidence in support of this assumption.[5,12,16–18] At the experimental site, a strong case for the power-law geoacoustic profile is made by Osler and Chapman[12] and by Chapman.[8] Figure 2 illustrates the model, and depicts the simple power-law profile ($z_1=0$) as well as a truncated power-law profile ($z_1>0$) formed by offsetting the singularity of the profile. For the simple power-law profile, note that when $\nu<1/2$, $\nabla\mu$ tends to infinity when μ tends to zero. This makes the approach of Robins,[4,19] who assumes slow variation of μ and discards terms with μ derivatives, inapplicable to the problem at hand.

Mathematically, an analytic treatment of the problem on noise resonances is made possible by the existence of two small parameters. The first one, Δ_1, is the ratio of Lame constants μ and λ in the soft sediment. At the experimental site it does not exceed 0.007. The second small parameter, Δ_2, is the ratio of the horizontal component of wave vector to the shear-wave wave number in the soft sediment. It follows from the Snell's law that, if the ambient noise sources are in the water column or at the ocean surface, Δ_2 is limited from above by the ratio of shear-wave velocity in the soft sediment to the sound speed in the water. If the ambient noise sources are situated deep in the bottom, Δ_2 does not exceed the ratio of shear-wave velocities in soft and hard sediments. At the site considered, for the second small parameter we have, respectively, upper bounds of 0.09 and 0.14. Related to Δ_2 is another small parameter, T, defined as the product of density and shear velocity ratios in soft and hard sediments at their interface. In this case, it is on the order of $T=0.1$.

At normal incidence ($\Delta_2=0$) and with $T=0$, the interfaces with the water and the hard sediment act like a free and a rigid boundary for shear waves in soft sediment, and there exist normal modes of shear waves with real frequencies f_n. At oblique incidence and/or when T is finite, the eigenfrequencies take on complex values because of radiation losses into the water and the hard sediment. However, variations in the eigenfrequencies compared to the ideal case $\Delta_2=T=0$ are small, including their imaginary parts, as long as Δ_2 and T are small. In the problem of broadband wave reflection from the sediment layer, the existence of complex eigenfrequencies near the real axis leads to frequency resonances. This can be demonstrated in several ways. First, compare the reflection problem for the continuous wave and the eigenvalue problem. In terms of the amplitudes of the four linearly independent *P-SV* waves in the layer, each problem reduces to a linear algebraic system. The only difference is, the algebraic system is homogeneous in the eigenvalue problem (free vibrations) but has a nonzero right hand side due to the incident wave in the reflection problem (forced vibrations). When the frequency f of the incident wave approaches an eigenfrequency, the determinant of the linear system tends to zero and, hence, solutions of the inhomogeneous system generally tend to infinity. Of course, with CW excitation, the amplitudes of the resonance peaks remain bounded because the eigenfrequencies are slightly complex.

For a more graphic explanation, consider a continuous plane sound wave incident on the layer $0<z<H$ of soft sediment from a fluid half-space $z<0$. Let $z=H$ be a rigid boundary. If the horizontal displacement in the incident wave is $U^{(in)}(z)$, then the horizontal displacement in P waves at $z=H$ is proportional to $U^{(in)}(H)$. (The coefficient of proportionality is 2 when P wave reflection above the boundary $z=H$ is negligible.) Let $u(z,f)$ stand for the horizontal dis-

placement in S waves as a function of depth and frequency. From the boundary condition of no horizontal displacement at $z=H$ it follows that $u(H,f)=\text{const}\,U^{(in)}(H)$. (The constant equals -2 when P wave reflection above the boundary $z=H$ is negligible.) On the other hand, $u(z,f)$ is proportional to one of the two linear-independent solutions for shear waves, say, $U^{(s)}(z,f)$ that obeys the boundary condition of no horizontal traction at $z=0$. Therefore, $u(z,f)=u(H,f)U^{(s)}(z,f)/U^{(s)}(H,f)=\text{const}\,U^{(in)}(H)U^{(s)}(z,f)/U^{(s)}(H,f)$. At an eigenfrequency $f=f_n$, the shear wave obeys the boundary conditions at *both* interfaces $z=0$ and $z=H$. Hence, $U^{(s)}(H,f_n)=0$. We now see that $u(0,f)$ tends to infinity when f tends to f_n and that resonant peaks in horizontal displacement are related to normal modes of shear waves. In reality, the height of the resonance peaks is large but limited because of the small shift of the eigenfrequency away from the real axis.

Consequently, although no normal mode is actually excited at plane-wave reflection, to determine the frequencies of noise resonances it is sufficient to study the eigenfrequencies of P-SV waves in the soft sediment layer. Prediction of the heights of the peaks is a more subtle issue as the heights depend on both imaginary parts of the eigenfrequencies and the noise power spectrum and directionality. In this paper, we will concentrate on the resonance condition, which determines positions of the resonance frequencies, leaving analysis of the heights of the peaks for further research.

III. THE EFFECT OF THE ANGLE OF INCIDENCE ON THE RESONANCE FREQUENCIES

Consider elastic P-SV waves in a stratified fluid/solid medium. The medium is infinite or has horizontal ideal (free or rigid) horizontal boundaries. The solid is assumed to be locally isotropic. Let $\mathbf{u}^{(\alpha)}$, $\sigma_{jk}^{(\alpha)}$, $\mathbf{q}^{(\alpha)}=(q_1^{(\alpha)},q_1^{(\alpha)},0)$, and ω_α be the displacement, stress tensor, horizontal wave vector, and frequency corresponding to two normal modes; $\alpha=1,2$; $j,k=1,2,3$. The fields of the normal modes are orthogonal in fluid/solid media. We express the orthogonality relation in the form[20]

$$\int dz[(\omega_1^2-\omega_2^2)\rho u_j^{(1)}u_j^{(2)} + i(q_\alpha^{(1)}-q_\alpha^{(2)})(\sigma_{j\alpha}^{(1)}u_j^{(2)}-\sigma_{j\alpha}^{(2)}u_j^{(1)})]=0. \quad (2)$$

Here the integration is performed throughout the vertical extent of the medium; summation over repeated indices is implied.

The orthogonality relation enables us to relate eigenfrequencies corresponding to two different values of the wave vector. At normal incidence, shear and compression waves are known to be uncoupled in layered solids (Ref. 21, Sec. 1.3). Let $\mathbf{q}^{(1)}=0$ (normal incidence), $\mathbf{q}^{(2)}=(q,0,0)$. Assume that the normal mode considered is a shear wave at $\mathbf{q}=0$. (It may have a P component at $\mathbf{q}\neq 0$.) Hence, $\mathbf{u}^{(1)}=(u_1^{(1)},0,0)$. According to the Hooke's law $\sigma_{jk}=\lambda\delta_{jk}\partial u_s/\partial x_s+\mu(\partial u_j/\partial x_k+\partial u_k/\partial x_j)$, where $j,k,s=1,2,3$; $\sigma_{j1}^{(1)}$ is nonzero only when $j=3$. Then one obtains from Eq. (2)

$$\omega^2(q)-\omega^2(q=0)=-iq\frac{\int dz[\sigma_{13}^{(1)}u_3^{(2)}-\sigma_{11}^{(2)}u_1^{(1)}]}{\int dz\rho u_1^{(1)}u_1^{(2)}}. \quad (3)$$

Of course, both eigenfrequencies in the left side are real in the absence of dissipative processes for normal modes in a solid layer with ideal boundaries and for proper normal modes in an unbounded medium. When the depth dependence of horizontal displacement is chosen to be real-valued, the integral in numerator on the right side of Eq. (3) is pure imaginary. As $u_3^{(2)}$ and $\sigma_{11}^{(2)}$ tend to $u_3^{(1)}$ and $\sigma_{11}^{(1)}$ and, hence, vanish at $q\to 0$, it follows from Eq. (3) that the eigenfrequency increment is proportional to q^2 for small q.

For comparison, consider the analogous expressions for shear waves of horizontal polarization (SH waves). These waves are not coupled to P-SV waves in layered solids and have zero vertical displacement at all angles of incidence. The horizontal component of displacement obeys the wave equation (Ref. 21, Sec. 1.3)

$$\frac{\partial^2 u}{\partial z^2}+\frac{1}{\mu}\frac{\partial\mu}{\partial z}\frac{\partial u}{\partial z}+(k^2-q^2)u=0,\quad k=\frac{\omega}{c},\quad c=\sqrt{\frac{\mu}{\rho}}, \quad (4)$$

where k is the shear-wave wave number. From Eq. (4) it follows [cf. Eq. (3)]

$$\omega^2(q)-\omega^2(q=0)=q^2\frac{\int dz\mu(z)u(q,z)u(0,z)}{\int dz\rho(z)u(q,z)u(0,z)}. \quad (5)$$

Expressing the integrals on the right side through depth-averaged values of shear modulus and density, one has

$$\omega^2(q)/\omega^2(q=0)=1+q^2\langle\mu\rangle/\omega^2(q=0)\langle\rho\rangle=1+O(q^2/K^2) \quad (6)$$

when $q\ll K$. Here K is a representative value of shear-wave wave number. Thus the relative change of the eigenfrequency of SH waves due to the variation of the horizontal wave number is of the order q^2/K^2 when q is small compared to the shear-wave wave number.

The same conclusion is valid for waves of vertical polarization as well. It can be demonstrated in two different ways. First, one can merely note that shearlike waves are supported even by an incompressible solid. Therefore, there exist elastic waves for which all the stress tensor components remain finite at $\lambda\to\infty$. In other words, all the stress tensor components are proportional to μ in these shearlike waves. Then $\sigma_{11}^{(2)}$ is on the order of $\mu q u_1^{(1)}$. Noting also that $\sigma_{13}^{(1)}$ and $u_3^{(1)}$ are on the order of $\mu k u_1^{(1)}$ and $q u_1^{(1)}/k$, respectively, one obtains the estimate Eq. (6) for *vertically* polarized waves from Eq. (3).

Alternatively, for a more formal derivation, one can apply the method of multi-scale expansions. Formally substituting $\epsilon^{-2}\lambda$ for λ and ϵq for q in the vector wave equation for P-SV waves (Ref. 21, Sec. 1.3.3) and developing the displacement vector into a power series in the formal small parameter ϵ, after equating coefficients at similar powers of ϵ, one arrives at a system of equations for zero, first, and higher order contributions to the displacement. For the sake of brevity, we omit details of the analysis and present the relevant findings only. It turns out that when $\epsilon\ll 1$, that is, in solids with $\mu\ll\lambda$, there are two types of elastic waves.

Waves of different type are uncoupled to leading order in ϵ. When div $\mathbf{u}$ is not small, the waves are essentially compressional, and shear rigidity results in small corrections only. For the other wave type, div $\mathbf{u}=O(\epsilon^2)$, that is, the displacement is almost purely rotational, as in a shear wave. Then, according to Hooke's law, $\sigma_{13}^{(1)}u_3^{(2)}$ and $\sigma_{11}^{(2)}u_1^{(1)}$ are on the order of $\mu q u_1^{(1)}$, and the estimate Eq. (6) follows from Eq. (3).

An important corollary of this result is that the relative variation in the frequency of the eigenmode due to variation of the angle of incidence is of the order of the square of the small parameter Δ_2. Therefore, under the environmental conditions at the experimental site, the spread of eigenfrequencies of a given normal mode due to various possible (real) incidence angles results in broadening of the respective spectral line in the power spectrum by a few percent at most. This is much less than width of spectral lines observed in the seismo-acoustic ambient noise. Hence, to determine eigenfrequencies it is sufficient to consider the case of the normal incidence only. At normal incidence *SV* and *SH* waves become indistinguishable.

IV. EXACT SOLUTIONS FOR THE POWER-LAW PROFILE

A. General solution

Consider elastic waves in a continuously stratified solid with constant density and a power-law profile Eq. (1) of the shear modulus with $z_1=0$. Written in terms of $\psi=\mu^{1/2}u$, the wave equation (4) for waves *SH* becomes the Helmholtz equation

$$\frac{d^2\psi}{dz^2}+K^2\psi=0,$$
$$K^2=\frac{\rho\omega^2}{\mu}-q^2+\left(\frac{1}{2\mu}\frac{d\mu}{dz}\right)^2-\frac{1}{2\mu}\frac{d^2\mu}{dz^2} \tag{7}$$

with effective wave number K. We are interested in the case $q=0$, when the same wave equation applies to *SV* waves.

In connection with reflection of acoustic and electromagnetic waves, exact solutions to the Helmholtz equation with effective wave number squared

$$K^2(z)=\tfrac{1}{4}b^2(z+z_1)^2[b^{-2}-4m^2+4lQ(z+z_1)^b$$
$$-Q^2(z+z_1)^{2b}] \tag{8}$$

have been studied in Ref. 21, Sec. 3.3, and Ref. 22. Such an equation is solvable in terms of confluent hypergeometric functions (Ref. 23, Chap. 13), the general solution being

$$\psi(z)=\eta^{(1-b)/2b}[A_1M_{l,m}(\eta)+A_2W_{l,m}(\eta)],$$
$$\eta=Q(z+z_1)^b, \tag{9}$$

where $M_{l,m}$ and $W_{l,m}$ are Whittaker functions and $A_{1,2}$ are arbitrary constants. Note that if $l=0$ the Whittaker functions reduce to the simpler and more frequently used cylindrical functions.

At $q=0$, the effective wave number in Eq. (7) for shear waves is the same as in Eq. (8) if parameters in Eq. (8) are chosen in the following way:

$$l=0,\quad m=\pm(1/2-\nu)/(1-\nu),\quad b=1-\nu,$$
$$Q=2i\omega c_0^{-1}/(1-\nu),\quad z_1=0. \tag{10}$$

Hence, at normal incidence and $\nu\neq 1$, the exact solution of the wave equation for shear waves is given by Eqs. (9) and (10). Taking into account the relations (Refs. 21, Sec. 3.3; 23, Chap. 13) between cylindrical functions and the Whittaker functions, it is convenient to re-write Eq. (9) as

$$u=z^{1/2-\nu}\left[B_1J_m\left(\frac{\omega}{c_0(1-\nu)}z^{1-\nu}\right)\right.$$
$$\left.+B_2Y_m\left(\frac{\omega}{c_0(1-\nu)}z^{1-\nu}\right)\right],$$
$$m=\frac{2\nu-1}{2(1-\nu)}, \tag{11}$$

where J_m and Y_m are the Bessel functions of the first and the second kind. Note that m is a monotonically increasing function of ν, and it varies between $-\frac{1}{2}$ and plus infinity when ν increases from 0 to 1. By using the Bessel equation (Ref. 23, Chap. 9), to which J_m and Y_m are solutions, it is straightforward to check by direct substitution that $u(z)$ as defined in Eq. (11) is a solution of the wave equation (4). We note in passing that exact closed-form solutions of the wave equation (7) can be also obtained from Eqs. (8) and (9) in the case of *oblique* incidence ($q\neq 0$), but only for the particular values ($\nu=-1$, 0, $\frac{1}{2}$, and 1) of the parameter ν.

B. A layer with ideal boundaries

Consider a sediment layer $0<z<H$ with constant density, a power-law profile Eq. (1) for the shear modulus, $z_1=0$, and the following boundary conditions (BCs) imposed on the layer boundaries:

$$\sigma_{13}=0\quad(z=0), \tag{12}$$
$$u_1=0\quad(z=H). \tag{13}$$

Physically, the BC at $z=0$ corresponds to the boundary with the (inviscid) fluid; the BC at $z=H$ corresponds to a rigid boundary.

From Hooke's law and the limiting forms of the Bessel functions for small arguments

$$J_m(\eta)=\Gamma^{-1}(1+m)(\eta/2)^m[1+O(\eta^2)],$$
$$Y_0(\eta)=2\pi^{-1}\ln z+O(1),$$
$$Y_M(\eta)=-\pi^{-1}\Gamma(M)(\eta/2)^{-M}[1+O(\eta^2)]+o(1), \tag{14}$$
$$M>0,$$

it follows that one should put $B_2=0$ in (11) to satisfy BC Eq. (12). Hence, the particle displacement in a normal mode is given by

$$u=B_1z^{1/2-\nu}J_m\left(\frac{\omega}{c_0(1-\nu)}z^{1-\nu}\right), \tag{15}$$

where B_1 is an amplitude constant. The displacement is bounded throughout the layer and is nonzero at the interface

$z=0$. The BC Eq. (13) immediately gives the resonance condition

$$J_m\left(\frac{\omega}{c_0(1-\nu)}H^{1-\nu}\right)=0. \tag{16}$$

Using the common designation $j_{m,n}$ (Ref. 23, Sec. 9.5) for the nth positive zero of the function $J_m(x)$, one has from the dispersion relation Eq. (16) the explicit expression

$$f_n=(2\pi)^{-1}c_0(1-\nu)H^{\nu-1}j_{m,n} \tag{17}$$

for the nth resonance frequency, $n=1,2,...$ All the resonance frequencies are real. It follows from the properties of the Bessel function zeros (Ref. 23, Sec. 9.5) that for a given ν the sequence $\{f_n\}$ is not generally equally spaced: $f_{n+1}-f_n \neq f_n-f_{n-1}$, but rapidly becomes so as n increases. At $n \gg 1+m^2$

$$f_n=\frac{c_0(1-\nu)}{2\pi H^{1-\nu}}\beta\left[1-\frac{4m^2-1}{8\beta^2}+O\left(\frac{1}{\beta^4}\right)\right],$$

$$\beta=\pi\left(n+\frac{m}{2}-\frac{1}{4}\right). \tag{18}$$

For instance, at $m=1$, substituting 1 for the square brackets in Eq. (18) results in errors in f_n that are less than 2.5% for the fundamental (lowest) mode ($n=1$) and less than 1% at $n\geqslant 2$. According to Eq. (18), the sequence of the resonance frequencies can only be spaced equally if $m^2=1/4$. That is, among the power-law profiles (other than the trivial case of μ constant) only the one with $\nu=\frac{3}{2}$ can possibly result in an equi-spaced set of resonance frequencies. As will be shown in a moment, in the case $\nu=\frac{3}{2}$, the sequence of the resonance frequencies is indeed equi-spaced and, furthermore, harmonic.

The general expressions Eqs. (15) and (17) for the resonance frequencies and field of the normal mode can be further simplified when m takes the half-integer values $m=M+\frac{1}{2}$ and, hence, $\nu=1-(2M+1)^{-1}$, where $M=0,1,2,...$ The Bessel functions of half-integer order are proportional to the spherical Bessel functions (Ref. 23, Chap. 10), which are in turn a combination of elementary functions. In particular,

$$J_{1/2}(\eta)=(2/\pi\eta)^{1/2}\sin\eta,$$

$$J_{3/2}(\eta)=(2/\pi\eta)^{1/2}(\eta^{-1}\sin\eta-\cos\eta), \tag{19}$$

$$J_{-1/2}(\eta)=-Y_{1/2}(\eta)=(2/\pi\eta)^{1/2}\cos\eta.$$

According to Eq. (19), at $\nu\to 0$ Eq. (15) gives the solution $u=\text{const}\cos(\omega z/c_0)$ which was certainly anticipated for the homogeneous layer with the boundary condition Eq. (12). At $\nu=\frac{3}{2}$, one has from Eqs. (15) and (19)

$$u=B_1\sqrt{\frac{2c_0}{3\pi\omega}}z^{-1/3}\sin\left(\frac{3\omega}{c_0}z^{1/3}\right). \tag{20}$$

Note that in this case the mode phase (argument of the sine) becomes zero at $z=0$ and not $\pi/2$, as one might expect by assuming similarity to the case of homogeneous layer. From Eq. (18) and BC Eq. (13) it is clear that the resonance frequencies form the harmonic sequence $f_n=\text{const}\cdot n$ in this case.

At $\nu=4/5$ it follows from Eqs. (15) and (19) that

$$u=B_1(2/\pi)^{1/2}(5\omega/c_0)^{-3/10}\eta^{-3}(\sin\eta-\eta\cos\eta),$$

$$\eta=5\omega c_0^{-1}z^{1/5}. \tag{21}$$

Now the normal mode field contains both sine and cosine components, with comparable and nearly mutually annihilating values at $z\to 0$.

C. Truncated power-law profile

Consider now a somewhat more general geoacoustic model. We retain the assumptions made in Sec. IV B about the problem geometry, constant density, boundary conditions, and normal incidence, but take z_1 to be positive in Eq. (1). The model will be referred to as *the truncated power-law profile*. Of primary interest to us is the effect that small but nonzero $\mu(0)$ has on the resonance frequencies.

The general solution of the wave equation is still given by Eq. (11) if $z+z_1$ is substituted for z in the right side of that equation. Using the identities

$$mJ_m(\eta)\mp\eta\,dJ_m(\eta)/d\eta=\eta J_{m\pm1}(\eta),$$

$$mY_m(\eta)\mp\eta\,dY_m(\eta)/d\eta=\eta Y_{m+1}(\eta), \tag{22}$$

BCs Eqs. (12) and (13) can now be written as

$$B_1J_{m+1}(a)+B_2Y_{m+1}(a)=0,\quad a=\omega z_1^{1-\nu}/c_0(1-\nu), \tag{23a}$$

$$B_1J_m(b)+B_2Y_m(b)=0,\quad b=\omega(H+z_1)^{1-\nu}/c_0(1-\nu). \tag{23b}$$

By requiring that these simultaneous equations have a nontrivial solution with respect to amplitude constants $B_{1,2}$, one obtains the resonance condition

$$J_{m+1}(a)Y_m(b)-J_m(b)Y_{m+1}(a)=0 \tag{24}$$

for shear waves in the "truncated" layer. Note that in Eq. (24) $b>a$ and $b\gg a$ when $z_1\ll H$. Using the limiting forms Eq. (14) of the Bessel function for small arguments, it is easy to verify that in the limit $z_1\to 0$ Eq. (24) reduces to the dispersion relation Eq. (16) for a nontruncated layer.

Consider two special cases:

1. The case $a\ll 1$

According to Eq. (23a), this is the case when z_1 or, in other words, the shear-wave velocity near the upper boundary of the sediment layer is sufficiently small. (As will become clear soon, the exact meaning of "sufficiently" depends on the mode number.) The inequality $z_1\ll H$ is a necessary, but generally not a sufficient condition for a to be much smaller than unity at a resonance frequency.

Note that $1+m>0$ for all possible ν values. It follows from Eq. (14) that $J_{m+1}(a)/Y_{m+1}(a)$ tends to zero when a tends to zero. Therefore $J_m(b)$ in the dispersion relation Eq. (24) is small when $a\ll 1$. Hence, b is close to a zero $j_{m,n}$ of the Bessel function. Using small argument forms for $J_{m+1}(a)$ and $Y_{m+1}(a)$ and developing $J_m(b)$ and $Y_m(b)$ into Taylor series in the vicinity of $b=j_{m,n}$, after some algebra one obtains from Eq. (24)

$$f_n=\frac{c_0(1-\nu)j_{m,n}}{2\pi(z_1+H)^{1-\nu}}\left[1+d_{m,n}\frac{z_1}{z_1+H}+O\left(\left(\frac{z_1}{z_1+H}\right)^{\gamma}\right)\right], \tag{25}$$

where $\gamma=\min(2,3-2\nu)$,

$$d_{m,n}=-\frac{2^{-2(m+1)}\pi j_{m,n}^{2m+1}}{(m+1)\Gamma^2(m+1)}\frac{Y_m(j_{m,n})}{J_m'(j_{m,n})}, \tag{26}$$

and prime denotes derivative of the function with respect to its argument. The expression for $d_{m,n}$ can be simplified in some cases. In particular, using Eq. (19) one finds $d_{1/2,n}=\pi^2n^2/3$ at $\nu=\frac{1}{3}$. At arbitrary m and large n the simple expression

$$d_{m,n}\sim\frac{\pi}{2(m+1)\Gamma^2(m+1)}\left[\frac{\pi}{2}\left(n+\frac{m}{2}-\frac{1}{4}\right)\right]^{2m+1} \tag{27}$$

is obtained by noting (Ref. 23, Sec. 9.2) $J_m'(j_{m,n})/Y_m(j_{m,n})=-1+O(n^{-2})$. Although Eq. (27) has been derived for large n, it turns out to be rather accurate even for $n=2$ when $m\leq 1$.

Written in terms of the ratio of shear-wave velocities at the top and bottom of the sediment layer, Eq. (25) becomes

$$f_n=\frac{c_0(1-\nu)j_{m,n}}{2\pi(z_1+H)^{1-\nu}}\left[1+d_{m,n}\left(\frac{c(0)}{c(H)}\right)^{1/\nu}+O\left(\left(\frac{c(0)}{c(H)}\right)^{\gamma/\nu}\right)\right]. \tag{28}$$

The expressions in the square brackets in Eqs. (25) and (28) represent a correction factor relating the resonance frequency for a truncated layer to that of the nontruncated layer *with the same shear-wave velocity at its bottom*. It should be emphasized that relative variation in the frequency is much less than the relative variation of wave travel time between the boundaries $z=0$ and $z=H$, the latter relative variation being $(1+H/z_1)^{\nu-1}$. If one compares resonance frequencies of the truncated and nontruncated layers *of the same thickness H*, then similar expressions hold. In particular,

$$f_n=\frac{c_0(1-\nu)j_{m,n}}{2\pi H^{1-\nu}}\left[1+(d_{m,n}-1+\nu)\left(\frac{c(0)}{c(H)}\right)^{1/\nu}+O\left(\left(\frac{c(0)}{c(H)}\right)^{\gamma/\nu}\right)\right]. \tag{29}$$

As the leading term in the correction factor in both cases is proportional to the (small) ratio $c(0)/c(H)$ of the shear-wave velocities to the power greater than unity, the resonance frequencies of the truncated layer are relatively insensitive to $c(0)$ for first normal modes. For instance, with $c(0)=7.5$ m/s, $c(H)=130$ m/s, from Eq. (28) one has 1.0456 and 1.182 for the ratio of resonance frequencies of truncated and nontruncated layers at $n=1$ and $n=2$ and $\nu=\frac{1}{3}$. At $\nu=\frac{1}{4}$, the ratios are 1.006 17, 1.0144, and 1.022 58 for $n=1$, $n=2$, and $n=3$, respectively. The smaller ν, the smaller are changes in the resonance frequencies and slower their increase with mode number. These properties of the resonance frequencies are illustrated in Sec. VI.

The coefficient $d_{m,n}$ increases with the normal mode order n as n^{2m+1} [see Eq. (27)] making Eqs. (28) and (30) inapplicable to high-order modes. An analysis shows that the restriction on mode number is determined by the inequality $a\ll 1$ which can be re-written with the help of Eq. (28) as $z_1/H\ll(\pi n)^{-1/(1-\nu)}$.

2. The case $a\gg 1+m^2$

When $z_1\ll H$, this case applies to high-order normal modes only. Using Hankel's asymptotic expansions (Ref. 23, Sec. 9.2)

$$\begin{aligned}&J_m(\eta)=(2/\pi\eta)^{1/2}[N(m,\eta)\cos\chi-M(m,\eta)\sin\chi],\\&\chi=\eta-\pi m/2-\pi/4,\\&Y_m(\eta)=(2/\pi\eta)^{1/2}[M(m,\eta)\cos\chi+N(m,\eta)\sin\chi],\\&N(m,\eta)\sim\sum_{k=0}^{\infty}(-)^k\frac{(m,2k)}{(2\eta)^{2k}},\\&M(m,\eta)\sim\sum_{k=0}^{\infty}(-)^k\frac{(m,2k+1)}{(2\eta)^{2k+1}}\end{aligned} \tag{30}$$

for the Bessel functions in Eq. (24), one finds, after some algebra,

$$\cos(b-a)+\sin(b-a)\left[\frac{4(m+1)^2-1}{8a}-\frac{4m^2-1}{8b}\right]+O(a^{-2}+b^{-2})=0. \tag{31}$$

The equation can be solved with respect to the frequency leading to

$$2\pi f_n\tau=\frac{\pi}{2}+\pi n+\frac{(H+z_1)^{1-\nu}-z_1^{1-\nu}}{8\pi(n+1/2)}\left[\frac{4(m+1)^2-1}{z_1^{1-\nu}}-\frac{4m^2-1}{(H+z_1)^{1-\nu}}\right]+O(n^{-2}), \tag{32}$$

where

$$\tau=\int_0^H\frac{dz}{c(z)}=\frac{(H+z_1)^{1-\nu}-z_1^{1-\nu}}{c_0(1-\nu)} \tag{33}$$

is wave travel time between the layer boundaries at normal incidence. Unlike the case in Sec. IV C 3, the relative variation in the resonance frequency due to truncation of the layer is approximately equal to the relative variation in wave travel time. One can recognize in terms $O(n)$ and $O(1)$ in Eq. (32) the WKB resonance condition (for the case of one free and one rigid boundary) whereas terms $O(1/n)$ represent leading-order corrections to the WKB approximation. The connection between Eq. (32) and the WKB resonance condition is not accidental; it will be shown in Sec. V that the inequality $a\gg 1+m^2$ ensures applicability of the WKB approximation throughout the truncated layer.

D. The effect of the boundary conditions

In the Secs. IV B and IV C above, ideal boundary conditions Eqs. (12), (13) have been assumed. While the first of these BCs is the correct BC for shear waves at normal incidence on a solid/fluid interface provided fluid viscosity and surface roughness are negligible, the second BC corresponds

to an absolutely rigid surface and is a strong idealization. Instead of imposing that BC at the boundary $z=H$, we now make a more realistic assumption that half-space $z>H$ is occupied by a homogeneous solid with density ρ_2 and shear-wave velocity c_2. At a solid/solid interface with a "welded" contact, shear waves at normal incidence are not coupled to compressional waves, and the physical requirements of displacement and traction continuity at the interface reduce to two boundary conditions, namely, continuity of the x-component of the displacement and of the σ_{13} component of the stress tensor. In the absence of waves coming from infinity, the displacement field in the half-space $z>H$ is given by

$$u_1=A\exp(i\omega z/c_2), \quad z>H, \quad A=\text{const}. \tag{34}$$

Therefore, $\sigma_{13}/u_1=i\omega\rho_2 c_2$ at the interface $z=H$. Continuity of u_1 and σ_{13} leads then to the following BC for waves within the sediment layer:

$$u_1+i\omega^{-1}cT\,\partial u_1/\partial z=0 \qquad (z=H), \quad \text{where} \quad T=\rho(H)c(H)/\rho_2 c_2 \tag{35}$$

and $\rho(H)$ and $c(H)$ are the density and shear-wave velocity in the layer just above the boundary with the solid half-space. We will assume $T\ll 1$. This is the case when shear-wave velocity in the "substrate" $z>H$ is much greater than in the sediment layer. T is the only parameter characterizing the effect of the substrate on the normal modes of the shear waves. In the limit $T\to 0$ Eq. (35) turns into Eq. (13). That is why the presence of the substrate with finite impedance can be considered as a perturbation with respect to the idealized problem with a rigid boundary.

Let us derive the resonance condition for shear waves in a layer between fluid and solid halfspaces. Imposing BC Eq. (35) on the solution Eq. (15) that meets the boundary condition at $z=0$, for the nontruncated layer one immediately obtains

$$J_m(\omega\tau)=iTJ_{m+1}(\omega\tau), \quad \tau=H^{\nu-1}/c_0(1-\nu). \tag{36}$$

As long as $T\ll 1$, $\omega\tau$ in Eq. (36) is close to a zero $j_{m,n}$ of the Bessel function. Developing $\omega\tau-j_{m,n}$ into a power series in T and using the identities $J_{m+1}(j_{m,n})=-J'_m(j_{m,n})$ and $J''_m(j_{m,n})=-J'_m(j_{m,n})/j_{m,n}$ [see Eq. (22)], after simple transformations one finds

$$f_n=\frac{c_0(1-\nu)}{2\pi}H^{\nu-1}\left[j_{m,n}-iT+\frac{1+2m}{2j_{m,n}}T^2+O(T^3)\right] \tag{37}$$

for the resonance frequencies. In the special cases $\nu=\frac{1}{3}$ ($m=\frac{1}{2}$) and $\nu\to 0$ ($m=-\frac{1}{2}$) the problem can easily be solved independently, without invoking cylindrical functions. Without presenting respective derivations, we note that the results obtained in the special cases agree with Eq. (37).

Comparison of Eq. (37) to Eq. (17) for the resonance frequencies in the case of a rigid lower boundary shows that penetrability of the boundary in the realistic model results in perturbations of both real and imaginary part of f_n. Because of the wave energy leakage through the boundary, the resonance frequencies cease to be real-valued. When $T\ll 1$, $\mathrm{Im}\,f_n$ is independent of mode number. With broadband excitation, the complexity of f_n manifests itself in the power spectrum as smearing of spectral lines, with the width of the lines (approximately) independent of their frequency. The term $O(T^2)$ in Eq. (37) is responsible for a shift of the spectral lines in the power spectrum. The shift is small, particularly if ν is small, and decreases as $1/n$ with mode number increasing. At $T<0.2$ and $m\sim 0.5$ the frequency shift does not exceed 0.41% even for the first normal mode and is practically negligible. Hence, the spectral line broadening is the only major effect of the finite impedance of the lower boundary of the nontruncated layer.

Consider now the truncated layer. Then the BC at the upper boundary leads to Eq. (23a), while the BC Eq. (35) becomes

$$[J_m(b)-iTJ_{m+1}(b)]B_1+[Y_m(b)-iTY_{m+1}(b)]B_2=0, \tag{38}$$

$$b=\frac{\omega}{c_0(1-\nu)}(H+z_1)^{1-\nu}$$

in terms of the unknown amplitude coefficients $B_{1,2}$. From the requirement that the linear simultaneous equations (23a) and (38) have a nontrivial solution with respect to $B_{1,2}$ one obtains the resonance condition

$$J_{m+1}(a)Y_m(b)-Y_{m+1}(a)J_m(b) =iT[J_{m+1}(a)Y_{m+1}(b)-Y_{m+1}(a)J_{m+1}(b)]. \tag{39}$$

It is a generalization of the dispersion equations (36) for the nontruncated layer with transparent lower boundary and Eq. (24) for the truncated layer with rigid lower boundary and reduces to those simpler relations in the limits $a\to 0$, $T\neq 0$ and $T\to 0$, $a\neq 0$, respectively.

Without delving into a detailed analysis of the dispersion relation Eq. (39), consider only one special case which is of primary practical interest. Namely, let $n=O(1)$, $a\ll 1$, $T\ll 1$. We will be interested in the leading-order corrections only with respect to the small parameters z_1 and T. Cast Eq. (39) as

$$J_m(b)=\frac{J_{m+1}(a)}{Y_{m+1}(a)}Y_m(b) +iT\left[J_{m+1}(b)-\frac{J_{m+1}(a)}{Y_{m+1}(a)}Y_{m+1}(b)\right]. \tag{40}$$

Developing the left side in powers of $b-j_{m,n}$ and the right side in powers of a and discarding terms $O(Tz_1)$, one finds

$$f_n\approx\frac{c_0(1-\nu)}{2\pi}(z_1+H)^{\nu-1}j_{m,n}\left[1+d_{m,n}\frac{z_1}{z_1+H}-\frac{iT}{j_{m,n}}\right], \tag{41}$$

where $d_{m,n}$ is defined in Eq. (26). Equation (41) describes perturbations in the resonance frequencies due to (i) finite impedance of the lower boundary and (ii) small but nonzero shear-wave velocity near the upper boundary. From Eq. (41) we see that, to leading order, the perturbations are additive as it should have been expected. These two perturbations have been already discussed above.

V. ASYMPTOTIC SOLUTIONS OF THE SHEAR-WAVE WAVE EQUATION

In this section we consider WKB and more advanced asymptotic approximations to solutions of the shear-wave equation at normal incidence. The results of Sec. IV will be extended to geoacoustic models with variable density and shear modulus profiles deviating from the power-law depth dependence.

A. WKB approximation and its conditions of use

Formal high-frequency asymptotic representation of the solutions of the wave equation (4) (with $q=0$) is

$$u=(\mu k)^{-1/2}(C_1e^{i\phi}+C_2e^{-i\phi})$$
$$=(\rho c)^{-1/2}(B_1\sin\phi+B_2\cos\phi),\quad \phi(z)=\omega\int_0^z\frac{dz'}{c(z')}. \tag{42}$$

where $B_{1,2}$ and $C_{1,2}$ are arbitrary constants, and ϕ is the phase integral. Equation (42) is the first approximation of the WKB method (Ref. 21, Sec. 8.1). The amplitude factor $\mu^{-1/2}$ in Eq. (42) stems from the term with the first derivative of u in Eq. (4). As long as $\mu\to 0$ at $z\to 0$, this factor dramatically changes the amplitude behavior of the solutions near the upper boundary of the layer.

The WKB asymptotic solutions are commonly interpreted as local plane waves, in which the phase ϕ is a much more rapidly varying function of position that the amplitude, the latter being $(\rho c)^{-1/2}$ in our case. The interpretation is justified as long as

$$\omega/c\gg|c^{-1}\,dc/dz|+|\rho^{-1}\,d\rho/dz| \tag{43}$$

This condition is often viewed as the applicability condition of the WKB approximation. For the power-law profile of the velocity and constant or slowly varying density, the condition Eq. (43) becomes $\omega\gg dc/dz=\nu c_0z^{\nu-1}$. When $\nu\geqslant 1$, this condition is met throughout the layer if it is met at $z=H$. On the contrary, at $\nu<1$ the condition is violated in a vicinity of $z=0$ no matter how large the wave frequency is. This highly peculiar behavior is brought about by the infinite value of the wave speed gradient at $z=0$.

For acoustic waves in fluids it is known (Ref. 21, Sec. 8.2) that in some cases the WKB solution can be close to or coincide with the exact solution even when wave amplitude is not a slowly varying function compared to its phase. As it will be shown below, such a situation is possible for shear waves as well. It is of considerable interest because of the great simplification of the analysis and interpretation for respective ν values.

Strict estimates of the deviation of the WKB solution from the exact solution are available in the case of the Helmholtz equation (see Ref. 21, Sec. 8.1 and references therein). In particular, let $W(s)$ be an exact solution to the equation

$$d^2W/ds^2+N^2(s)W(s)=0,\quad N^2(s)>0, \tag{44}$$

and let

$$w_{1,2}(s)=N^{-1/2}(s)\exp\left(\pm i\int_0^s N(s_1)ds_1\right) \tag{45}$$

be its two WKB solutions. Then, if $W(s)$ and one of the functions $w_{1,2}$ have equal values and equal first derivatives at some point $s=s_0$, the relative error of the WKB solution obeys the inequality

$$|\delta(s)|\leqslant e^{F(s,s_0)}-1,\quad F(s,s_0)=2\left|\int_{s_0}^s\epsilon(s_1)N(s_1)ds_1\right|, \tag{46}$$

where

$$\epsilon(s)=0.5N^{-3/2}d^2N^{-1/2}/ds^2. \tag{47}$$

Remarkably, the exact solution and its WKB asymptotics coincide when $N^{-1/2}$ is a linear function of s.

According to Eq. (46), the smallness of ϵ (more precisely, validity of the inequality $|N\epsilon|\ll 1$ for all s considered) is a sufficient condition of the WKB approximation applicability. On the other hand, taking second and third WKB approximations into account, one obtains (Ref. 21, Sec. 8.1)

$$u=(\rho c)^{-1/2}\exp\left(-\frac{\epsilon}{2}\pm i\omega\int_0^z\frac{dz'}{c}(1+\epsilon)\right) \tag{48}$$

instead of Eq. (42). Therefore, smallness of ϵ is also a necessary condition for the use of Eq. (42).

To apply these results to shear waves, we transform the wave equation (4) into the Helmholtz equation by introducing instead of z a new independent variable $s(z)$ according to the equation[24,25] $ds/dz=\mu_0/\mu$, where μ_0 is a constant. In terms of the new vertical coordinate s, the wave equation (4) (with $q=0$) becomes the Helmholtz equation

$$d^2u/ds^2+\mu_0^{-2}\rho\omega^2\mu u=0. \tag{49}$$

It is the same as Eq. (44) with $W=u$ and $N^2=\mu_0^{-2}\rho\omega^2\mu$. Designate $\mu_0=\rho_0c_0^2H^{2\nu}$; ρ_0 is a constant which in the case of depth-independent density we are considering is conveniently chosen as equal to ρ; H stands for the layer thickness. Then one has the following explicit expressions for $s(z)$:

$$s(z)=(1-2\nu)^{-1}H^{2\nu}z^{1-2\nu},\quad \nu>0,\quad \nu\neq 1/2;$$
$$s(z)=H\ln(z/H),\quad \nu=1/2. \tag{50}$$

When z increases from 0 to plus infinity, s increases: from 0 to plus infinity, if $0<\nu<\frac{1}{2}$, from minus infinity to plus infinity, if $\nu=\frac{1}{2}$, or from minus infinity to 0, if $\nu>\frac{1}{2}$.

Calculation of the quantities ϵ and F for $\nu\neq 1$ using Eqs. (46), (47), and (50) gives simple expressions

$$\epsilon(s(z))=\frac{\nu(2-3\nu)c_0^2}{8\omega^2}z^{2\nu-2},$$
$$F(s(z),s(z_0))=\left|\frac{\nu(2-3\nu)c_0}{4(1-\nu)\omega}(z^{\nu-1}-z_0^{\nu-1})\right|. \tag{51}$$

We see that when $0<\nu<1$, $\epsilon\to\infty$ and the error of the WKB approximation increases indefinitely when $z\to 0$ making the approximation meaningless. The only exception, according to Eq. (51) occurs when $\nu=\frac{3}{4}$. Then ϵ is identically zero, and the WKB solution is not just a good approximation but is *precisely equal* to the exact solution. The finding can be verified directly by comparing the WKB solution as defined by Eq. (42) with $\nu=\frac{3}{4}$ to the exact solution Eq. (11) where

cylindrical functions of the order $m=\frac{1}{2}$ are given by Eq. (19). What cannot be verified by collating the two solutions but follows immediately from Eq. (47) is that the power-law profile with $\nu=\frac{3}{2}$ is *the only case* of continuously stratified, inhomogeneous solid of constant density when WKB solutions are exact for shear waves at normal incidence.

With ν, z_0, and wave frequency given, Eqs. (46) and (51) allow one to estimate the vicinity of the horizon $z=z_0$ in which one can use the WKB approximation. We will restrict ourselves to the case $\nu=\frac{3}{2}+\delta$, $|\delta|\ll 1$. It is of primary interest for two reasons. First, according to Eq. (51), it is a favorable case when applicability domain of the WKB approximation is larger than usual. (The other favorable case is that of small ν, $\nu\ll 1$, that is, of weakly inhomogeneous medium. It could be considered in a similar way but is of little interest in the problem of the ambient noise resonances.) Second, ν values in the geoacoustic model fitting available experimental data are close to $\frac{3}{2}$.[8,12]

In the problem of normal modes in the sediment layer it is natural to choose $z_0=H$. Then the contribution to F from the term with z_0 in Eq. (51) is much smaller than unity and can be neglected at the fundamental resonance and higher frequencies. The condition of the WKB approximation validity, $|F|\ll 1$, to within linear terms in δ becomes $\delta\omega c_0 z^{-1/3}\ll 1$. Using Eq. (17) for the resonance frequencies, we cast the condition as

$$z/H\gg\delta^3/n^3. \tag{52}$$

Hence, at the fundamental frequency ($n=1$) the WKB approximation is valid in the entire layer with the exception of a narrow range in the vicinity of the boundary $z=0$. The vertical extent of this range is of the order $10\delta^3 H$ and decreases rapidly, as n^{-3}, with increasing mode number. For instance, at $\delta=0.07$ the vertical extent is within 0.35% of the total layer thickness H for the fundamental mode. In terms of the shear wave velocity and the phase integral Eq. (42), the condition Eq. (52) becomes $c(z)/c(H)\gg\delta/n$ or $\phi(z)\gg\delta$. In the case of a truncated layer, the WKB approximation applies throughout the layer if $c(0)/c(H)\gg\delta/n$. For example, with $c(H)=130$ m/s, $n=2$, and $\delta=0.07$ this condition is met if $c(0)\gg 18$ m/s.

So far the WKB approximation has been analyzed in the case when an exact solution is available. The real value of the WKB approximation consists, of course, in its ability to treat efficiently a much wider class of environmental models than those admitting an exact analytic solution. To illustrate this point, we briefly consider three examples.

(1) Let the shear modulus be given by the power-law Eq. (1) with $z_1=0$ and $\nu=\frac{3}{2}$ in the layer with depth-dependent density $\rho(z)$. The layer is situated between homogeneous fluid ($z<0$) and solid ($z>H$) half-spaces. It is assumed that $\rho>0$, is a smooth function of z, and varies slowly with depth compared to the wave field, that is

$$|\rho^{-1}\,d\rho/dz|\ll\omega/c(H),\quad |\rho^{-1}\,d^2\rho/dz^2|\ll\omega^2/c^2(H). \tag{53}$$

The latter assumption is met for all the normal modes, if the representative space scale L of ρ variation is large compared to H or if $\rho(z)=\rho_0+\delta\cdot\rho_1(z)$, where ρ_0 and δ are constants, $\delta\ll 1$, and the representative space scale of ρ_1 variation is of the order of H. For any smooth $\rho(z)$, condition Eq. (53) holds for modes of order high enough, namely, with $n\gg H/L$. Note that because of the density depth-dependence shear wave velocity $c(z)$ does not follow a power law.

With arbitrary smooth $\mu(z)$ and $\rho(z)$, for ϵ one has from Eq. (47)

$$\epsilon=-\frac{\mu}{8\rho\omega^2}\left[\frac{d^2}{dz^2}\ln\rho-\frac{1}{4}\left(\frac{d}{dz}\ln\rho\right)^2+\frac{d^2}{dz^2}\ln\mu+\frac{3}{4}\left(\frac{d}{dz}\ln\mu\right)^2+\frac{1}{2}\left(\frac{d}{dz}\ln\rho\right)\left(\frac{d}{dz}\ln\mu\right)\right]. \tag{54}$$

For the power-law profile of $\mu(z)$ and $\nu=\frac{3}{2}$, the terms without ρ in the square brackets in Eq. (54) equal zero. Then $\epsilon\to 0$ at $z\to 0$, and, because of Eq. (53), $|\epsilon|\ll 1$ throughout the layer and $|F(s(z),s(H))|\ll 1$. Therefore, the WKB approximation is valid at $0<z<H$.

The general solution of the wave equation is given by Eq. (42). For the displacement to be finite at $z\to 0$ one has $B_2=0$ in Eq. (42). Imposing the BC Eq. (35) at the lower boundary, one obtains the resonance condition

$$\tan\phi(H)=-iT\left[1-\frac{iT}{2\omega}\left(c'(H)+c(H)\frac{\rho'(H)}{\rho(H)}\right)\right]^{-1}. \tag{55}$$

This equation is easily solved when $T\ll 1$:

$$f_n=\frac{n}{2\tau}\left[1-\frac{iT}{\pi n}+\frac{\tau T^2}{2\pi^2 n^2}\left(c'(H)+c(H)\frac{\rho'(H)}{\rho(H)}\right)+O(T^3)\right], \tag{56}$$

where τ is wave travel time between layer boundaries. Noting that $j_{1/2,n}=\pi n$, it is straightforward to check that Eq. (56) reduces to Eq. (37) in the particular case of the depth-independent density. Like its counterpart Eq. (37) derived from the exact solution, Eq. (56) describes both broadening of the spectral line due to energy leakage at the solid/solid interface and a small shift of the spectral line compared to the case of rigid boundary ($T=0$). Equation (56) shows that observations made in Sec. IV D hold for a more general geoacoustic model.

In the case of a rigid lower boundary Eq. (55) gives the harmonic sequence $f_n=n/2\tau$ of the resonance frequencies. For a *homogeneous* layer with the same value of travel time τ and the same boundary conditions one gets $f_n=(2n+1)/4\tau$, which is not harmonic. The difference occurs because the free surface BC at the upper boundary leads to the *different choice of solutions* when $c(0)=0$ and $c(0)\neq 0$. Indeed, when $c(0)\neq 0$, to meet the BC one has to choose the solution with $\cos\phi$ in Eq. (42) When $c(0)=0$, both sine and cosine solutions give $\sigma_{13}=0$ at $z=0$ but only the sine solution is bounded, leading to $B_2=0$ and $f_n=n/2\tau$.

Put differently, the harmonic sequence of the resonance frequencies results from the fact the wave equation (4) for the shear waves *is not* a Helmholtz equation. It is the amplitude factor $\mu^{-1/2}$ in the WKB solution Eq. (42) that is responsible for the distinction in the resonance frequencies of the inhomogeneous and homogeneous layers with the same τ. The amplitude factor, in its turn, originates from the term with the first derivative of u in the wave equation (4).

(2) Let us consider two elastic layers sandwiched between homogeneous fluid ($z<0$) and solid ($z>H+h$) half-spaces. In the layer $0<z<H$, $\mu(z)$ follows the power law with $v=\frac{3}{2}$. In the layer $H<z<H+h$, $\mu(z)$ is an arbitrary smooth function varying slowly compared to the wave field. Density is a smooth function of z at $0<z<H+h$, varying slowly compared to the wave field. Density and shear modulus are continuous at $z=H$ together with their first derivatives.

Then the WKB approximation is applicable at $0<z<H+h$, and one gets the same resonance condition for the shear waves, as in case (1) above, with τ being now travel time between the boundaries $z=0$ and $z=H+h$. We see, that elastic layers with the same τ and the same type of μ singularity at $z\to 0$ have very similar dispersion curves. (Additional examples of such a behavior are given in Sec. V B below.) In practice, therefore, no unique inversion of the resonance frequencies for the shear modulus depth dependence is possible, even within the class of monotonic $\mu(z)$ and with many resonance frequencies measured.

(3) Consider an elastic layer with the BCs Eqs. (12), (13) imposed on its boundaries. Let $\mu>0$ at $z=0$ and throughout the layer, μ and ρ be smooth functions of depth, and the wave frequency be high enough so that the WKB approximation is valid at $0<z<H$. Calculating the derivative of Eq. (42) with respect to z and neglecting terms $O(1/n)$ compared to 1, one obtains from the BCs Eqs. (12), (13) the resonance condition $\cos(\phi(H)-\phi(0))=0$, or $f_n=(2n+1)/4\tau$, where τ is the wave travel time between the boundaries $z=0$ and $z=H$. The dispersion relation, within its accuracy, agrees with the dispersion relation Eq. (32) derived from the exact solution and extends it to the case of arbitrary smooth variation of the medium parameters. Note that the shear-wave dispersion relation is no different from the dispersion relation for acoustic waves in a fluid layer with one free and the other rigid boundary *provided* the shear modulus does not turn to zero within the elastic layer or on its boundary.

B. Uniform asymptotics

The WKB method enables one to derive high-frequency asymptotics of solutions to the wave equation with an *arbitrary* smooth depth dependence of medium parameters, but, as discussed in Sec. V A, with a few exceptions is not applicable in a vicinity of the horizon where the shear modulus vanishes. The exact solutions considered in Sec. IV have no limitations on frequency or depth but refer to media with $\rho=\text{const}$ and specific $\mu(z)$. In this section, we derive an asymptotic representation that possesses virtues of both the approaches mentioned.

As before, we assume normal incidence. Let $\mu=\rho(z)c^2$, $c=F(z)z^{\nu}$; ρ and F are smooth functions with L being the representative spatial scale of their variation: $F'/F=O(L^{-1})$, $\rho'/\rho=O(L^{-1})$. Neither F nor ρ vanishes within the layer. In this geoacoustic model, the shear modulus retains its power-law singularity at $z\to 0$, but can deviate from the power law considerably at $z\gtrsim L$.

To derive a wave field asymptotics applicable at $z\to 0$, we apply the *reference equation method* (see Ref. 21, Chap. 9 and references therein). The exactly solvable wave equation for the power-law $\mu(z)$ dependence will serve as the "reference equation." Let $W(s)$ be a solution of Eq. (44) in the reference case. Then the function

$$U(s)=(d\eta/ds)^{-1/2}W(\eta(s)) \tag{57}$$

obeys the equation (Ref. 21, Sec. 9.1)

$$\begin{aligned} &d^2U/ds^2+[(d\eta/ds)^2N^2+P(s)]U=0,\\ &P(s)=0.5(\ln\eta')''-0.25[(\ln\eta')']^2, \end{aligned} \tag{58}$$

where prime denotes derivatives with respect to s. Generally, the variable substitution $\eta(s)$ is chosen from the following two conditions: (i) $(\eta')^2N^2$ equals to the coefficient $\mu_0^{-2}\rho\omega^2\mu$ in the Helmholtz equation (49) to be solved, and (ii) positions and types of "critical points" (i.e., zeros and singularities) in the coefficients of Eqs. (49) and (58) coincide. In the problem at hand, there is a single critical point, $z=0$, where coefficients of Eq. (49) and the reference equation have power-law singularities.

For brevity, only the case $\frac{1}{2}<\nu<1$ will be considered below. Then $s\to-\infty$ at $z\to+0$ [see Eq. (50)], and the appropriate variable substitution is

$$\int_{-\infty}^{\eta}N(\eta')d\eta'=\frac{\omega}{\mu_0}\int_{-\infty}^{s}[\rho(s')\mu(s')]^{1/2}ds'. \tag{59}$$

Calculating the integrals, one finds

$$\begin{aligned} &\eta(s)=\operatorname{sgn}(1-2\nu)\left|\frac{\phi}{2\alpha m}\right|^{-2m},\\ &\alpha=\frac{\omega}{c_0H^{2\nu}}\left|\frac{1-2\nu}{H^{2\nu}}\right|^{\nu/(1-2\nu)}, \end{aligned} \tag{60}$$

with ϕ defined in Eq. (42). Taking $W(s)$ as the general solution of the reference problem, after some algebra one obtains from Eqs. (11), (57), and (60) a concise expression

$$U=(\phi/\rho c)^{1/2}[B_1J_m(\phi)+B_2Y_m(\phi)], \tag{61}$$

where $B_{1,2}$ are arbitrary constants. Note that U, like the WKB solutions Eq. (42), is expressed in terms of the phase integral and ρ and c values at the point considered, but, unlike the WKB solutions, also depends on the exponent ν which determines m by Eq. (11). According to Eq. (61), with $c(z)$ given, the only effect of the density stratification on U is multiplication by the amplitude factor $\text{const}\cdot\rho^{-1/2}$. For comparison, the situation is similar with acoustic waves in fluids (Ref. 21, Sec. 9.1) but the factor is $\text{const}\cdot\rho^{1/2}$ in that case.

The function $U(s)$ Eq. (57) is an asymptotic solution to the wave equation, *if* the ratio

$$R=\frac{P(s)}{(d\eta/ds)^2N^2(s)} \tag{62}$$

is small with respect to the parameter L for all the coordinate s values considered (Ref. 21, Sec. 9.1). Using Eqs. (58) and (60) to calculate R, one finds

$$R=\frac{F^2(z)z^{2\nu}}{2\omega^2}\left[(\ln\rho Fg)''+(\ln\rho Fg)'(\ln\rho F^2)''\right.$$
$$\left.+\frac{2\nu}{z}(\ln\rho Fg)'-\frac{1}{2}((\ln\rho Fg)')^2\right], \tag{63}$$

where $g(z)=z^{\nu}[\phi(z)]^{-\nu/(1-\nu)}$. It is a smooth function with the same spatial scale L as $F(z)$; in particular, $g'(0)/g(0)=\nu(2-\nu)^{-1}F'(0)/F(0)$. Therefore, one can cast Eq. (63) as

$$R=\frac{F^2}{\omega^2}[z^{2\nu}O(L^{-2})+\nu z^{2\nu-1}O(L^{-1})]$$
$$=\frac{C_1(z/L)^{2\nu}+C_2(z/L)^{2\nu-1}}{k^2(L)L^2}, \tag{64}$$

where $C_{1,2}$ are dimensionless constants on the order of 1 and $k(z)$ is a wave number. Note that $R\to 0$ at $z\to 0$, $R\simeq(k(L)L)^{-2}$ at $z\gtrsim L$, and $R\ll(k(L)L)^{-2}$ at $z\ll L$. [We assume that the power-law increase of $c(z)$ ceases at some $z\gtrsim L$ and, therefore, do not consider the case $z\gg L$.] Hence, if

$$k(L)L\gg 1, \tag{65}$$

Eqs. (57) and (61) are applicable at any z and, then, Eq. (61) is a uniform asymptotics. As Eq. (65) is the condition of the WKB approximation applicability away from the singularity, the uniform asymptotics extends the WKB result up to the boundary $z=0$ *without any additional assumptions or additional restrictions on the wave frequency*. At the resonance frequency, according to Eq. (17), $k(H)H\simeq n$. Hence, with $L\lesssim H$ the uniform asymptotics Eq. (61) generally applies to high-order modes ($n\gg 1$) only. It applies to all normal modes if (i) $L\gg H$ or (ii) $\rho=\rho_0+\delta\cdot\rho_1(z)$ and $F=F_0+\delta\cdot F_1(z)$, where $\delta\ll 1$, ρ_0, and F_0 are constants and L is the spatial scale of ρ_1 and F_1 variation. In both cases the deviation of density from a constant and shear velocity from the power law are small within the layer. (That is not surprising, for one needs a small parameter to construct an approximation valid for all the modes.)

As expected, Eq. (61) reduces to the exact solution Eq. (11) when density is constant and $F=$const. It follows from Eq. (19) that the uniform asymptotics turns into the WKB solution Eq. (42) when $m=\frac{1}{2}$. Moreover, using the asymptotic expansions Eq. (30) of the Bessel functions it is easy to verify that for arbitrary m Eq. (61) reduces to the WKB solutions far away from the boundary $z=0$, namely, when $\phi\gg 1+m^2$.

A similar analysis can be carried out when $0<\nu<\frac{1}{2}$. However, it turns out that it that case R Eq. (62) tends to *infinity* at $z\to 0$, and Eq. (61) is generally not a uniform asymptotics. This fact is best understood by considering the wave equation in the form Eq. (7). The effective wave number in Eq. (7) contains $\rho'c'/\rho c$ and other terms $O(1/zL)$ which have a stronger singularity at $z\to 0$ than $\omega^2c_0^{-2}z^{-2\nu}$ when $\nu<\frac{1}{2}$. These terms change the asymptotic behavior of the solution at $z\to 0$ and call for a reference equation different from the one we used. If the first derivatives of both ρ and F become zero at $z=0$, then the indicated difficulty disappears, $R\to 0$ at $z\to 0$, and Eq. (61) turns out to be a uniform asymptotic in the case $0<\nu<\frac{1}{2}$ as well.

Now, let us use Eq. (61) to derive a resonance condition for shear waves in a layer $0<z<H$ between homogeneous fluid and solid half-spaces. For the displacement u to be finite at $z\to 0$, $B_2=0$ in Eq. (61). Imposing the BC Eq. (35) at $z=H$ and taking Eq. (65) into account, one obtains the resonance condition Eq. (36) where τ stands for the wave travel time between the boundaries $z=0$ and $z=H$. The only difference from the exactly solvable case involves the value of τ which now is not related to H and ν in as simple way as in Eq. (36). There is no need therefore to discuss anew the solution of the resonance condition. It is worth mentioning that the asymptotic derivation of the resonance condition extends conclusions made in Sec. IV D (without changing them) about effects of boundary conditions on the resonance frequencies to more general geoacoustic models.

Quite similarly one can derive from Eq. (61) a resonance condition in the case of truncated layer. We will not present the derivation here.

Consider the resonance condition Eq. (36) in the case $T=0$ (rigid lower boundary). Then the resonance frequencies are $\omega_n=j_{m,n}/\tau$. Using the asymptotic expansion for the Bessel function zeros (Ref. 23, Chap. 9) one has at $n\gg 1$ [cf. Eq. (18)]

$$\omega_n=\frac{\pi}{\tau}\left(n+\frac{m(\nu)}{2}-\frac{1}{4}\right)+O\left(\frac{1}{n}\right). \tag{66}$$

In the case $m=\frac{1}{2}$ Eq. (66) is exact for all $n=1,2,\ldots$. Compare Eq. (66) to the formal WKB resonance condition $\omega_n=\pi n/\tau$. At $m\neq\frac{1}{2}$ inapplicability of the WKB approximation in the vicinity of the boundary $z=0$ deletes the term $\pi(m/2-1/4)$ on the right side of the formal WKB result. The phase term $\pi(m/2-1/4)$ is analogous to the term $-\pi/4$ in the case of a turning point (Ref. 21, Sec. 9.2) but, because of its m dependence, is different for different media. Naturally, the phase term vanishes at $m=\frac{1}{2}$ when the WKB approximation is exact.

VI. DATA ANALYSIS AND COMPUTATIONAL EXAMPLES

The analysis so far provides valuable insight into the physics of the observed noise resonances. Here we reconsider the experimental noise data in light of the analytical results and we present some calculations based on the derived formulas to illustrate their applicability.

First we consider the simple power-law profile (i.e., nontruncated, with $z_1=0$) with a perfectly rigid lower boundary. The resonance frequencies for this case are expressed in terms of the zeros of Bessel functions in Eq. (17). For a shear wave at normal incidence, the two-way travel time through the upper sediment layer is $2H^{1-\nu}/c_0(1-\nu)$, so we normalize all frequencies by the reference frequency

$$F=(1-\nu)c_0/2H^{1-\nu}. \tag{67}$$

This is not the frequency of the fundamental resonance (except in the special case $\nu=\frac{2}{3}$), but in the limit of large mode order it is the frequency spacing of adjacent resonances, and

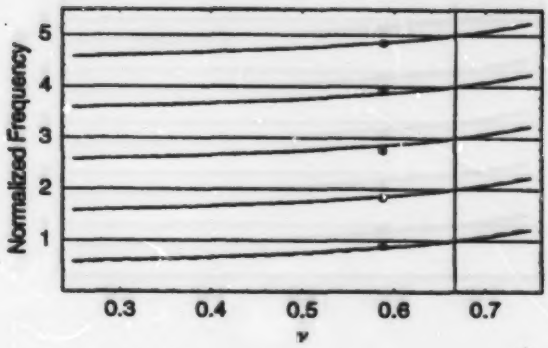

FIG. 3. Normalized resonance frequencies f_n/F vs exponent value ν in the shear-speed profile $c=c_0z^\nu$ with a rigid bottom boundary for shear resonances 1–5. The reference frequency F is defined by Eq. (67). Solid lines: exact solution; dashed lines: asymptotic approximation Eq. (66); thin horizontal lines: WKB approximation; solid circles: observed resonances, normalized by $F=1.18$ Hz.

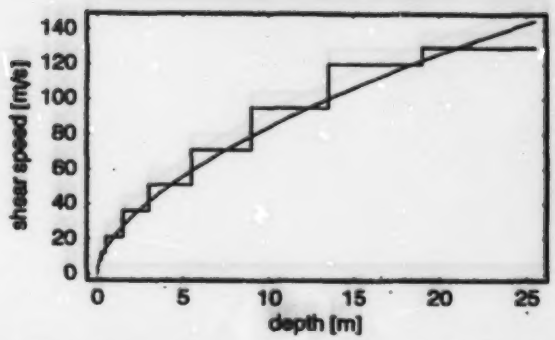

FIG. 4. The experimental shear-speed profile. The staircase is the stacked-layer profile previously derived from interface wave dispersion and the continuous line is the power-law profile $c(z)=21.7z^{0.59}$ (SI units) implied by the noise resonances. See text for more details.

we will show that it is a very good approximation even for low mode order.

Figure 3 shows the normalized shear resonance frequencies versus ν for the first five modes, calculated three different ways: (1) ignoring terms of $1/n$ and higher powers in Eq. (66) asymptotically valid for high-order modes; (2) by numerical solution of the exact normal mode resonance condition; and (3) by the WKB approximation $f_n=nF$. For method (2), the FindRoot function of Mathematica® is employed to solve Eq. (16) using f_n from method (1) as starting values. These two methods have nearly identical results, the only perceptible difference occurring at low mode order. The separation of adjacent normalized frequencies is very close to unity, but the offset of the sequence of resonances is clearly ν-dependent. Note that the resonance frequencies are exactly harmonic in the special case $\nu=\frac{1}{3}$. Note also that in the limit $\nu\to 0$, which corresponds to a homogeneous layer, the sequence of normalized frequencies approaches $n-\frac{1}{2}$. Method (3), the WKB approximation, was shown in Sec. V to apply only in the case $\nu=\frac{1}{3}$, in which case it is exact. In terms of normalized frequencies, the WKB resonance frequencies are simply the sequence of integers, n.

The precision of the asymptotic approximation Eq. (66) allows a straightforward reduction of the experimental data reported in Sec. I. To first order in $1/n$, Eqs. (66) and (17) can be written as $f_n=F(n+m/2-1/4)$, which is applied to the sequence of five noise resonances to determine the free parameters by linear regression. The resulting fit gives $F=1.18$ and $m=0.21$, which corresponds to the shear speed profile parameters $c_0=21.7\pm1.5$ and $\nu=0.59\pm0.06$. The experimental resonance frequencies, normalized by $F=1.18$, have been added to Fig. 3, plotted at the exponent value $\nu=0.59$. The good agreement between experimental and modeled resonances supports the hypothesis that the observed noise peaks are shear-wave resonances in a sediment layer having a power-law shear-speed profile. (It should be emphasized, however, that two shear-speed profiles having the same two-way travel time and power-law singularities of the shear speed at $z\to 0$ with the same ν cannot be distinguished by their resonance frequencies.) Owing to the natural uncertainties in the experimental data, no further improvement in the agreement is expected by introducing complicating factors, such as a truncated profile or a nonideal bottom boundary condition.

The implied power-law shear-speed profile is nearly identical to that independently determined from analysis of interface wave dispersion at the same site, discussed in Ref. 12 and reported in Sec. I. The continuous profile inferred from the seismo-acoustic noise analysis is plotted in Fig. 4 along with the stacked-layer "staircase" of shear-speed values used in the interface wave study. (It must be emphasized that the noise resonances being examined in this paper are modes of vibration of the sediment layer that are distinct from the interface waves studied in Ref. 12, although they are related through the common shear-speed profile.) It is satisfying that the power-law profile implied by the noise resonances is consistent with the profile derived from the interface-wave studies.

Figure 5 shows three power-law profiles having different exponents ν but the same two-way travel time, that is, they all have the same reference frequency F. The exponent values are $\nu=\frac{1}{4}$, $\nu=\frac{1}{2}$, and $\nu=\frac{2}{3}$. For each profile, Fig. 6 shows the shapes of the first three resonances in this ideal environment, assuming a perfectly rigid boundary at the bottom. The functions describing horizontal displacement are given by

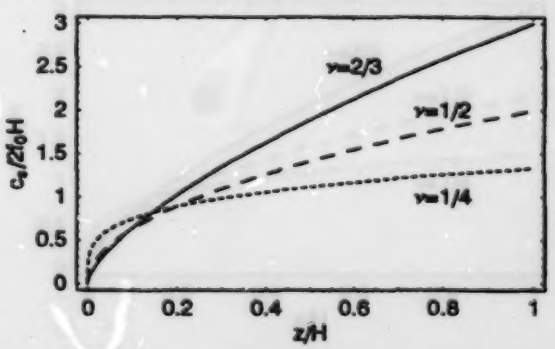

FIG. 5. Shear speed versus depth for power-law profiles having different exponential parameters, keeping fixed the two-way travel time through the layer.

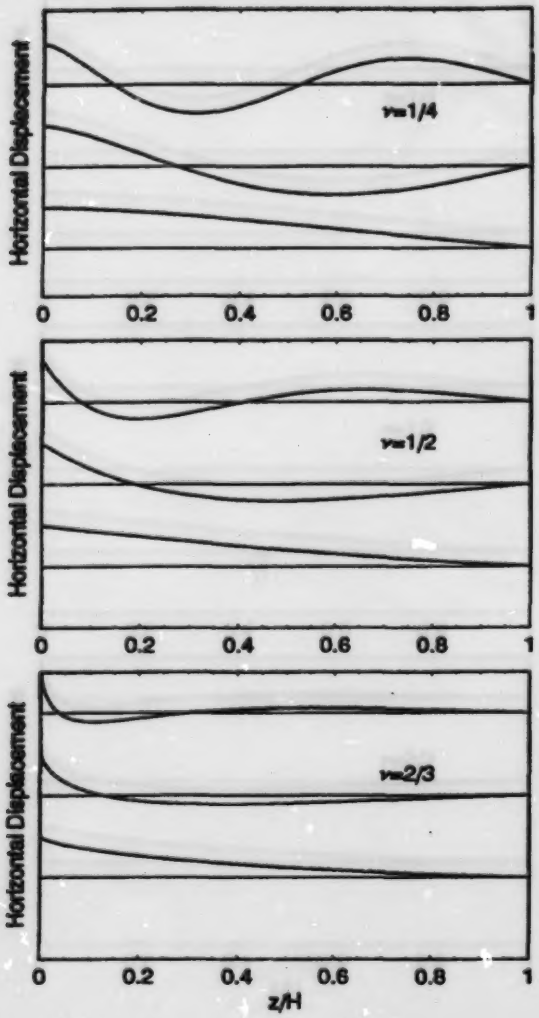

FIG. 6. Shapes of the first three shear-wave resonances associated with the profiles of Fig. 4. The zeros of the functions are offset by their normalized resonance frequencies.

Eq. (15), normalized to unity at the upper boundary, and are evaluated at the resonance frequencies given by Eq. (17). Note that at large values of the exponent the modes are trapped near the surface, while at small values of the exponent the modes span the sediment layer. In the limit $\nu \to 0$, the layer becomes isospeed and one would expect cosinusoidal mode shapes. The modes for the experimental case, having the exponent $\nu = 0.59$, are very similar to those for the case $\nu = \frac{2}{3}$.

Finally, we present an example of the resonance frequencies for the truncated power-law profile, whose resonance condition is Eq. (24). The numerical solutions of this equation were again found using the FindRoot function of Mathematica®, with starting values given by the corrected WKB approximation in Eq. (33). Computed for the case $z_1/H = 0.01$, the resonance frequencies given by these two methods are compared in Fig. 7 alongside the results from the simple (nontruncated) profile having the same parameters. Note that the truncated profile gives higher frequencies, owing to the reduced travel time through the sediment. The WKB approximation improves with mode order, as expected.

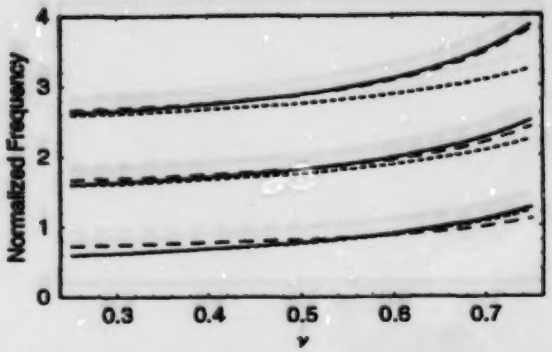

FIG. 7. Normalized resonance frequencies versus exponent value ν in the truncated shear-speed profile $c = c_0(z+z_1)^\nu$ with a rigid bottom boundary for shear resonances 1–3. The reference frequency is given by Eq. (67) and $z_1/H = 0.01$. Solid lines: exact solution; long dashed lines: the corrected WKB approximation, Eq. (33); short dashed lines: the nontruncated solution (as a reference).

VII. DISCUSSION AND CONCLUSIONS

Noise peaks in the spectra of seismo-acoustics signals observed on an ocean bottom seismometer have been interpreted as resonances of vertically polarized shear waves in a surficial layer of soft sediment overlaying a hard substrate, with the shear speed in the sediment layer increasing with depth according to a power law of the form $c(z) = c_0 z^\nu$ with $c_0 = 21.7 \pm 1.5$ (SI units) and $\nu = 0.59 \pm 0.06$. This profile agrees with that suggested by inversion of interface wave group speed data at the same experimental site. The noise resonances are related to quasi-modes of *P-SV* waves trapped in the sediment layer. Particle motion in these modes is dominated by the horizontal shear displacement. This is consistent with the absence of resonances in the observed noise spectra of the pressure sensor (the hydrophone) and with the resonances being much more pronounced on the horizontal geophone compared with the vertical geophone.

The shear-wave resonances are natural modes of vibration of this environment and their characteristics are independent of the level and origin of the noise. Rather, the mode frequencies and shapes are determined by seismo-acoustic propagation within the layered sediment. In our theoretical analysis, we have been able to circumvent the complicated problem of continuous *P-S* coupling in solids having inhomogeneous elastic properties. The very small shear speeds in the sediment layer permit the simplifying assumption that the modal frequencies are independent of the incidence angle of the exciting wave. Hence, although oblique incidence is necessary to couple the incident sound wave to shear waves in the sediment, one can determine the resonance frequencies by considering the normal-incidence case, reducing the problem to the solution of a well-known scalar wave equation. Furthermore, the insensitivity of the resonance frequencies to incidence angle is essential to our hypothesis if the noise

source is thought to be the diffuse infrasonic ambient noise field in the ocean overhead. Otherwise, the peaks would be smeared out in frequency and would not be observed.

Assuming normal incidence, constant density, and a power-law shear-speed profile, exact solutions have been obtained for eigenfrequencies and modes in terms of Bessel functions of real order between $-\frac{1}{2}$ and plus infinity. In general, the resonance frequencies are not harmonic, or even equally spaced, although they are precisely equally spaced for $\nu=0$ and $\nu=\frac{1}{3}$, and exactly harmonic for $\nu=\frac{1}{2}$. However, a uniform asymptotic approximation (that is, a corrected WKB approximation) predicts nearly equal spacing and provides a workable estimate of the exact resonance frequencies for all mode orders.

Theoretically, the continuous variation of the shear speed introduces into the wave equation a term involving the logarithmic derivative of the shear modulus, distinguishing our problem from the analogous acoustical problem. This is critically important for the correct description of the field behavior in the vicinity of the surface, where the shear speed vanishes in a singular manner. The combined effects of this term and the upper boundary conditions remain significant even away from the interface, where the critical term is locally small compared to other terms in the wave equation. The net effect of the singular profile is a ν-dependent frequency shift of the resonances. It would not be possible to explain the nearly harmonic sequence of the experimentally observed noise peaks without accounting for the effect of the logarithmic derivative term.

Strictly speaking, the existence of the shear-speed singularity at the sediment invalidates the WKB method for this problem, and it is no surprise that the resonance frequencies predicted by the WKB method are generally impractical. However, for the special case of $\nu=\frac{1}{2}$, the WKB method is exact! A uniform asymptotic approximation, obtained by the method of reference equation, proves to be a better approach. In effect, this provides a corrected WKB approximation that is surprisingly good. The uniform asymptotics possess advantages of both the exact solution and the WKB approximation: like the WKB approximation, it applies to rather general smooth variation of the medium parameters but, like the exact solution, it remains valid when the shear modulus vanishes according to the power law.

In the problem considered, the resonance frequencies are primarily determined by two characteristics, namely, the two-way travel time of shear waves in the sediment layer and the exponent ν, which governs the type of shear-speed singularity. In practice, if only resonance frequencies are measured, there is a little hope to distinguish between two distinct geoacoustic models sharing the same values of these parameters. Of some importance are also elastic parameters of the substrate and—in the case of the truncated power-law profile—the surface value of the shear modulus. Some of the broadening of the noise peaks is attributed to the finite contrast between the sediment and substrate properties. Further research would be required to theoretically explain the shapes of the resonance peaks in the noise spectrum measured as well as the relation between spectra of vertical and horizontal displacements and near-bottom pressure.

ACKNOWLEDGMENTS

The authors are grateful to Dave Heffler of the Atlantic Geoscience Center/Bedford Institute of Oceanography for the loan of the OBS used on the sea test that discovered the seismo-acoustic noise resonances and to N. Ross Chapman of School of Earth and Ocean Sciences/University of Victoria for stimulating discussions. The contribution of John Osler to the DREA OBS project was invaluable. The Department of National Defense and the Natural Sciences and Engineering Research Council of Canada have supported this work.

[1] J. M. Hovem, M. D. Richardson, and R. D. Stoll, Eds., *Shear Waves in Marine Sediments* (Kluwer, Dordrecht, 1991).

[2] S. J. Hughes, D. D. Ellis, D. M. F. Chapman, and P. R. Staal, "Low-frequency acoustic propagation loss in shallow water over hard-rock seabeds covered by a thin layer of elastic-solid sediment," J. Acoust. Soc. Am. **88**, 283–297 (1990).

[3] F. B. Jensen, "Excess attenuation in low-frequency shallow-water acoustics: A shear wave effect?," in *Shear Waves in Marine Sediments*, edited by J. M. Hovem, M. D. Richardson, and R. D. Stoll (Kluwer, Dordrecht, 1991), pp. 421–430.

[4] A. J. Robins, "Generation of shear and compression waves in an inhomogeneous elastic medium," J. Acoust. Soc. Am. **96**, 1669–1676 (1994).

[5] M. V. Hall, "Acoustic reflectivity of a sandy seabed: A semianalytic model of the effect of coupling due to shear modulus profile," J. Acoust. Soc. Am. **98**, 1075–1079 (1995).

[6] J. A. Orcutt, C. S. Cox, A. C. Kibblewhite, W. A. Kuperman, and H. Schmidt, "Observations and causes of ocean and seafloor noise at ultra-low and very-low frequencies," in *Natural Physical Sources of Underwater Sound*, edited by B. R. Kerman (Kluwer, Dordrecht, 1993), pp. 203–232.

[7] A. C. Kibblewhite and C. Y. Wu, *Wave Interactions as a Seismo-acoustic Source* (Springer-Verlag, Berlin, 1996).

[8] D. M. F. Chapman, "Shear speed gradients and resonances in ocean seismo-acoustic modelling," in *Theoretical and Computational Acoustics '97*, edited by Y. C. Teng *et al.* (World Scientific, Singapore, 1999), pp. 147–158.

[9] D. M. F. Chapman, J. C. Osler, W. C. Risley, and J. C. Dodds, "Underwater acoustic measurements with a digital ocean bottom seismometer," J. Acoust. Soc. Am. **96**, 3330(A) (1994).

[10] D. J. Dodds, D. M. F. Chapman, J. C. Osler, and W. C. Risley, "Minimizing instrument effects in an ocean bottom seismometer," Can. Acoust. **22**, 161–162 (1994).

[11] J. C. Osler, D. M. F. Chapman, W. C. Risley, and J. C. Dodds, "*In situ* calibration of the coupling of an ocean bottom seismometer to sand and clay surficial sediments," EOS Trans. Am. Geophys. Union **75**, 419 (1994).

[12] J. C. Osler and D. M. F. Chapman, "Seismo-acoustic determination of the shear-wave speed of surficial clay and silt sediments on the Scotian Shelf," Can. Acoust. **24**, 11–22 (1996).

[13] L. H. King, *Surficial Geology of the Halifax-Sable Island Map Area, Marine Science Paper 1* (Department of Energy, Mines and Resources, Ottawa, 1970).

[14] L. M. Dorman, A. E. Schreiner, L. D. Bibee, and J. A. Hildebrand, "Deep-water sea-floor array observations of seismo-acoustic noise in the eastern Pacific and comparisons with wind and swell," in *Natural Physical Sources of Underwater Sound*, edited by B. R. Kerman (Kluwer, Dordrecht, 1993), pp. 165–174.

[15] N. R. Chapman and D. M. F. Chapman, "A coherent ray model of plane-wave reflection from a thin sediment layer," J. Acoust. Soc. Am. **94**, 2731–2738 (1993).

[16] E. I. Hamilton, "Attenuation of shear waves in marine sediments," J. Acoust. Soc. Am. **60**, 334–338 (1976).

[17] J. E. White, *Underground Sound Application of Seismic Waves* (Elsevier, Amsterdam, 1983), pp. 67–68.

[18] T. Iwasaki and F. Tatsuoka, "Effects of grain size and grading on dynamic shear moduli of sands," Soils Found. **17**, 19–35 (1997).

[19]A. J. Robins, "Plane-wave reflection from a solid layer with nonuniform density, sound speed, and shear speed," J. Acoust. Soc. Am. **103**, 1337–1345 (1998).
[20]O. A. Godin, "Acoustic mode reciprocity in fluid/solid systems: Implications on environmental sensitivity and horizontal refraction," in *Theoretical and Computational Acoustics '97*, edited by Y. C. Teng *et al.* (World Scientific, Singapore, 1999), pp. 59–76.
[21]L. M. Brekhovskikh and O. A. Godin, *Acoustics of Layered Medium. I: Plane and Quasi-Plane Waves* (Springer-Verlag, Berlin, 1990 and 1998).
[22]O. A. Godin, "On plane waves reflection by a stratified halfspace," Dokl. Akad. Nauk SSSR **255**, 1069–1072 (1980).
[23]M. Abramowitz and I. A. Stegun, Eds., *Handbook of Mathematical Functions with Formulas, Graphs, and Tables*, Appl. Math. Ser., Vol. 55 (National Bureau of Standards, Washington, 1964).
[24]S. O. Coen, "On the elastic profiles of a layered medium from reflection data. Part 1. Plane-wave sources," J. Acoust. Soc. Am. **70**, 172–175 (1981).
[25]O. A. Godin, "On a modification of the wave equation for a layered medium," Wave Motion **7**, 515–528 (1985).

#512278